Available online at www.sciencedirect.com
SCIENCE DIRECT
Journal of Sound and Vibration 292 (2006) 788–801
JOURNAL OF SOUND AND VIBRATION
www.elsevier.com/locate/jsvi

Numerical analysis and engineering application of large parameter stochastic resonance

Yong Gang Leng[a,*], Yong Sheng Leng[b], Tai Yong Wang[a], Yan Guo[c]

[a]School of Mechanical Engineering, Tianjin University, Tianjin 300072, China
[b]Department of Chemical Engineering, Vanderbilt University, Nashville, Tennessee 37235, USA
[c]School of Management, Tianjin University, Tianjin 300072, China

Received 17 May 2005; received in revised form 16 August 2005; accepted 5 September 2005
Available online 18 January 2006

Abstract

Under the condition of large parameters, it is difficult in signal processing to use the small parameter stochastic resonance (SR) approach to detect a weak signal submerged in strong noise from the response power spectrum of a bistable system. We develop a new method, the re-scaling frequency stochastic resonance (RFSR) to solve this technical issue. In practical applications, the RFSR method requires that the ratio of sampling frequency to the signal frequency be equal to or larger than 50. The input and the output signal-to-noise ratios of the bistable system demonstrate the effectiveness of the RFSR method. Finally, two practical cases, the monitoring and diagnosis of mechanical faults and the vibration analysis of metal cutting show that the RFSR approach is suitable for detecting an early fault and extracting weak signals from strong noise. Thus, the RFSR technique has potential applications in the engineering signal processing.

1. Introduction

When noise is added to a system, the output of the system usually deteriorates in quality. However, in some systems, adding a proper amount of noise will enhance the system output or response, rather than decrease it. This is currently the so-called stochastic resonance (SR). In signal processing, SR is commonly described as an increase in the signal-to-noise ratio (SNR) at the output of a nonlinear system. This is obtained through varying the noise level while keeping the input signal constant [1–3]. SR has been proposed as a useful means for signal processing in a wide variety of systems [1–8], including bistable systems [1,2], excitable systems [7], threshold systems [3,8], and biological systems [1,6]. Currently, there have been many theoretical developments of SR in conventional bistable systems [1,5,9–12]. However, the majority of the theoretical studies in this area have been focusing on low frequency and weak periodic signals masked by small noise, i.e., small parameter signals (the frequency and amplitude of a periodic signal and noise intensity are all smaller than one). This may be explained by the fact that most of the studies were restricted by adiabatic approximation and linear response theory, where these parameters were assumed to be small. Nevertheless,

*Corresponding author. Tel.: +86 022 27408118; fax: +86 022 27404536.
E-mail addresses: zeyangang@tdme.tju.edu.cn, zeyangang@yt-public.sd.cninfo.net (Y.G. Leng).

0022-460X/$ - see front matter © 2005 Elsevier Ltd. All rights reserved.
doi:10.1016/j.jsv.2005.09.040

periodic driving with large parameters (frequency and/or amplitude and/or noise intensity can be much larger than one) in real world can be often encountered. For example, the frequencies of mechanical faults of rotating machinery are usually much higher than one. The case of a strong periodic driving with large amplitude and weak noise was discussed in the literature [13,14]. However, the noise was significantly suppressed in a certain frequency range. In the present paper, the opposite case of a high frequency and weak periodic signal hidden in strong noise will be investigated. Here the "weak" means small compared to the noise level. By the proposal of a novel method of re-scaling frequency stochastic resonance (RFSR), an SR-like spectral spike at the frequency of the weak periodic signal can be obtained in the output spectrum of a dynamic bistable system. The advantage of the proposed method is that it can detect a weak signal in the presence of strong noise or of the same frequency noise (which is the part with spectra close to the input frequency [15]). In our numerical studies, the data length is limited based on the practical signal processing. Usually, short data processing is different from the data analysis of non-limited length. In principle, if the data length is sufficiently long, for any small amplitude of a periodic input, it is possible to obtain the first spectral peak of the periodic forcing using traditional methods, such as spectral analysis or averaging. Our work concentrates on the numerical study of the behavior of the large parameter bistable RFSR. Two examples of practical engineering application are provided to illustrate the effectiveness of the proposed RFSR technique in signal processing.

2. The small parameter SR of a bistable system

2.1. The general model

The three basic ingredients of producing SR phenomenon are: (1) a bistable or multistable system, (2) a weak coherent input (such as a periodic signal), and (3) a source of noise that is inherent in the system, or that adds to the coherent input. For a convenient description, consider the overdamped motion of a Brownian particle in a bistable potential in the presence of noise and a periodic forcing

$$\dot{x}(t) = -U'(x) + A_0 \sin(2\pi f_0 t + \varphi) + n(t), \tag{1}$$

where $U(x)$ denotes the reflection-symmetric quartic potential

$$U(x) = -\tfrac{1}{2}ax^2 + \tfrac{1}{4}bx^4. \tag{2}$$

Eq. (1) can be written as

$$\dot{x}(t) = ax - bx^3 + A_0 \sin(2\pi f_0 t + \varphi) + n(t), \tag{3}$$

where $n(t) = \sqrt{2D}\xi(t)$ with $\langle n(t)n(t+\tau)\rangle = 2D\delta(t)$. Here, D is the noise intensity and $\xi(t)$ presents a zero-mean, unit variance Gaussian white noise. a and b are real parameters. A_0 is the periodic signal amplitude and f_0 is the modulation frequency (angular frequency $\Omega = 2\pi f_0$). Eq. (3) is the nonlinear Langevin equation for one variable. In terms of an appropriate change of variables $x(t) \to \sqrt{a/b}x(t)$, $t \to at$, $A_0 \to A_0\sqrt{a^3/b}$, $f_0 \to f_0/a$, $D \to Da^3/b$, the potential or system parameters a and b can be eliminated such that Eqs. (2) and (3) can be written in the dimensionless form

$$U(x) = -\tfrac{1}{2}x^2 + \tfrac{1}{4}x^4, \tag{4}$$

$$\dot{x}(t) = x - x^3 + A_0 \sin(2\pi f_0 t + \varphi) + n(t). \tag{5}$$

The potential minima in scaled units are located at $\pm x_m$, with $x_m = 1$. The height of the potential barrier between the minima is given by $\Delta U = \frac{1}{4}$. Eq. (3), a bistable system subject to sinusoidal signal and white noise, is a simple model extensively investigated in the nonlinear science community.

2.2. The periodic response analysis

For convenience, we choose the phase of the periodic driving $\varphi = 0$, i.e., the input signal reads explicitly as $A(t) = A_0 \sin(2\pi f_0 t)$. The mean value $\langle x(t)|x_0, t_0\rangle$ is obtained by averaging the inhomogeneous process $x(t)$ with initial condition $x_0 = x(t_0)$ over the ensemble of the noise realizations. Asymptotically ($t_0 \to -\infty$), the

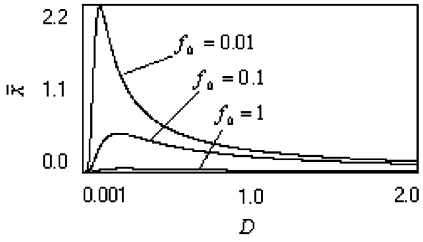

Fig. 1. The periodic response amplitude $\bar{x}$ vs. the noise strength D at a fixed modulation amplitude $A_0 = 0.3$ for different values of the frequency f_0 with $a = 1$, $b = 1$ in Eq. (3).

memory of the initial conditions gets lost and $\langle x(t)|x_0, t_0\rangle$ becomes a periodic function of time, i.e., $\langle x(t)\rangle_{as} = \langle x(t + T_f)\rangle_{as}$ with $T_f = 1/f_0$. For small amplitudes, the response of the system to the periodic input signal can be written as

$$\langle x(t)\rangle_{as} = \bar{x}\,\sin(2\pi f_0 t - \bar{\varphi}), \tag{6}$$

with amplitude $\bar{x}$ and a phase lag $\bar{\varphi}$. Approximate expressions for the amplitude and phase shift read as

$$\bar{x} = \frac{A_0\langle x^2\rangle_0}{D}\,\frac{r_k}{\sqrt{r_k^2 + \pi^2 f_0^2}}, \tag{7a}$$

$$\bar{\varphi} = \arctan\left(\frac{\pi f_0}{r_k}\right), \tag{7b}$$

where r_k is Kramers rate [1]

$$r_k = \frac{1}{\sqrt{2\pi}}\exp\left(-\frac{\Delta U}{D}\right), \tag{7c}$$

and $\langle x^2\rangle_0$ is the D-dependent variance of the stationary unperturbed system ($A_0 = 0$). Eq. (7) has been shown to hold in leading order of the modulation $A_0 x_m/D$ for both discrete and continuous one-dimensional systems [9,16,17]. Within two-state, Eq. (7) allows approximation $\langle x^2\rangle_0 = x_m^2$.

The most important feature of the amplitude $\bar{x}$ is that it depends on the noise strength D, i.e., the periodic response of the system can be manipulated by changing the noise level. We note from Eq. (7) that the amplitude $\bar{x}$ first increases with increasing noise level, reaches a maximum, and then decreases again. This is the celebrated SR effect shown in Fig. 1. At a closer inspection of Eq. (7a) and Fig. 1, it is also important to note that the variation of the frequency f_0 for fixed noise intensity D does not yield a resonance-like behavior of the response amplitude. The behavior of $\bar{x}$ versus f_0 for fixed noise D generally follows a monotonically decreasing trend. The response amplitude $\bar{x}$ goes to very small number with the increase of f_0. This indicates that SR phenomenon requires a low driving frequency, i.e., a small parameter frequency is necessary to an SR.

2.3. Power spectral density analysis

The power spectral density $S(f)$ commonly reported in the literature is the Fourier transform of the autocorrelation function. Instead of taking the ensemble average of the system response, it may be more convenient to extract the relevant phase-averaged power spectral density $S(f)$, defined here as

$$S(f) = \int_{-\infty}^{+\infty} \mathrm{e}^{-\mathrm{i}2\pi f\tau}\langle\langle x(t+\tau)x(t)\rangle\rangle\,\mathrm{d}\tau, \tag{8}$$

where the inner brackets denote the ensemble average over the realizations of the noise, and the outer brackets indicate the average over the input initial phase φ. Qualitatively, $S(f)$ may be described as the superposition of a background power spectral density $S_N(f)$ and a structure of delta spikes centered at $f = (2n + 1)f_0$ ($n = 0, \pm1, \pm2, \ldots$). The generation of only odd higher harmonics of the input frequency is typical fingerprints of periodically driven symmetric nonlinear systems. Since the strength (i.e., the integrated

power) of such spectral spikes decays with n according to a power law such as A_0^{2n}, we can restrict ourselves to the first spectral spike, being consistent with the linear-response assumption implicit in Eq. (6). For small forcing amplitudes, $S_N(f)$ does not deviate much from the power spectral density $S_N^0(f)$ of the unperturbed system. For a bistable system with relaxation rate $2r_k$, the hopping contribution of $S_N^0(f)$ reads as

$$S_N^0(f) = r_k\langle x^2\rangle_0/(r_k^2 + \pi^2 f^2). \tag{9}$$

The spectral spike at f_0 was verified experimentally [18–20] to be a delta function, thus signifying that there is a periodic component with frequency f_0 in the system response [Eq. (6)]. In fact, for $A_0 x_m \ll \Delta U$ we are led to separate $x(t)$ into a noisy background (which coincides, apart from a normalization constant, with the unperturbed output signal) and a periodic component with $\langle x(t)\rangle_{as}$ given by Eq. (6). On adding the power spectral density of either component, $S(f)$ is easily obtained as

$$\begin{aligned} S(f) &= (\pi/2)\bar{x}^2[\delta(f - f_0) + \delta(f + f_0)] + S_N(f) \\ &= \frac{\pi}{2}\left(\frac{A_0 x_m}{D}\right)^2 \frac{r_k^2 x_m^2}{r_k^2 + \pi^2 f_0^2}[\delta(f - f_0) + \delta(f + f_0)] + \left[1 - \frac{1}{2}\left(\frac{A_0 x_m}{D}\right)^2 \frac{r_k^2}{r_k^2 + \pi^2 f_0^2}\right] \frac{r_k x_m^2}{r_k^2 + \pi^2 f^2}. \end{aligned} \tag{10}$$

In fact, $S_N(f)$ is the product of the Lorentzian curve obtained with no input signal ($A_0 = 0$) and a factor that depends on the forcing amplitude A_0. Lorentzian distribution is characterized by concentrating most of noise energy into the low frequency region. That is, white noise energy distributing uniformly in traditional FFT frequency domain will mostly be accumulated into the low frequency region by the nonlinear bistable system. The behavior of $S_N(f)$ at $A_0 = 0$ versus frequency f is depicted for different noise intensity in Fig. 2. It is observed that increasing noise intensity widens the low frequency region, but shortens the amplitude of $S_N(f)$. We conclude that an SR spectral peak at f_0 should be confined at this energy-concentrated low-frequency region, since only a certain amount of noise can drive the particle over the potential barrier of the bistable system to form a transition SR. If the signal frequency f_0 is moved out of the low-frequency region, the SR effect will deteriorate or diminish at large frequencies.

To make this point clear, Figs. 3 and 4 show two examples. The relative parameters corresponding to the Langevin equation (3) in Fig. 3 are $A_0 = 0.3, f_0 = 0.01, D = 0.31, \varphi = 0, a = b = 1$ and noise $n(t) = \sqrt{2D}\xi(t)$, $\xi(t)$ denotes Gaussian white noise with zero-mean and one-variance. Sampling frequency is $f_s = 5$. The power spectral density $S(f)$ is calculated only with 1024 data points. The data length in time domain is 4000 points for a better view. Eq. (3) is numerically solved with a fourth-order Runge–Kutta method. The time step is $\Delta t = 1/f_s = 0.2$.

In Fig. 3, we can see clearly the typical SR phenomenon at the output of the bistable system. The sharp SR spectral spike at the modulation frequency f_0 is just located in the low-frequency region in which most noise energy concentrates. If the frequency f_0 is gradually increased to depart from the low frequency region whereas other parameters in Fig. 3 are held unchanged, the height of the output spectral spike at f_0 becomes smaller. This can be seen more evident in Fig. 4. The spectral height at $f_0 = 0.1$ in Fig. 4(a) is smaller than that at $f_0 = 0.01$ in Fig. 3, and the spectral height at $f_0 = 0.3$ in Fig. 4(b) is smaller than that at $f_0 = 0.1$ in Fig. 4(a). This result is also consistent with the results in Fig. 1, i.e., the SR phenomenon requires a small parameter frequency.

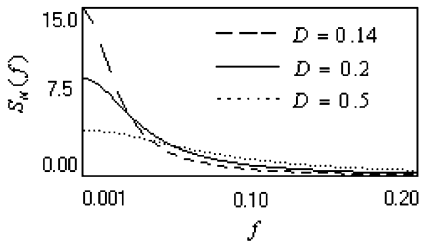

Fig. 2. The noise spectrum $S_N(f)$ in the symmetric bistable wells vs. frequency at the absence of driving force ($A_0 = 0$) for three values of the noise intensity D.

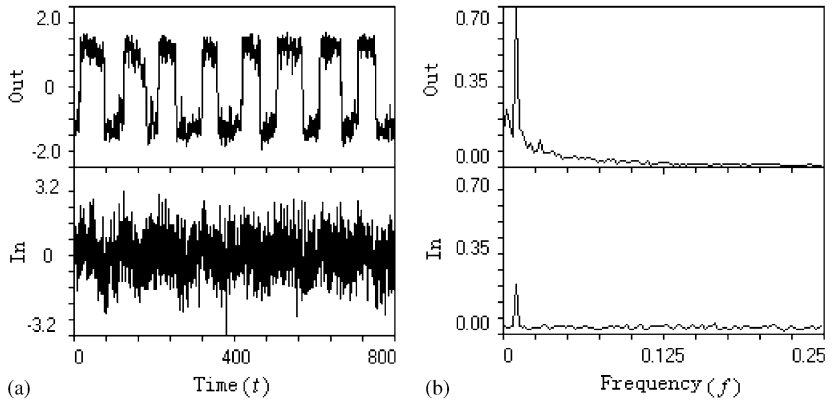

Fig. 3. Example of the input and output of the symmetric bistable system of Eq. (3). The relative parameters are $A_0 = 0.3$, $f_0 = 0.01$, $D = 0.31$, $\varphi = 0$, $a = b = 1$. (a) Time domain waveforms. (b) Frequency domain power spectra.

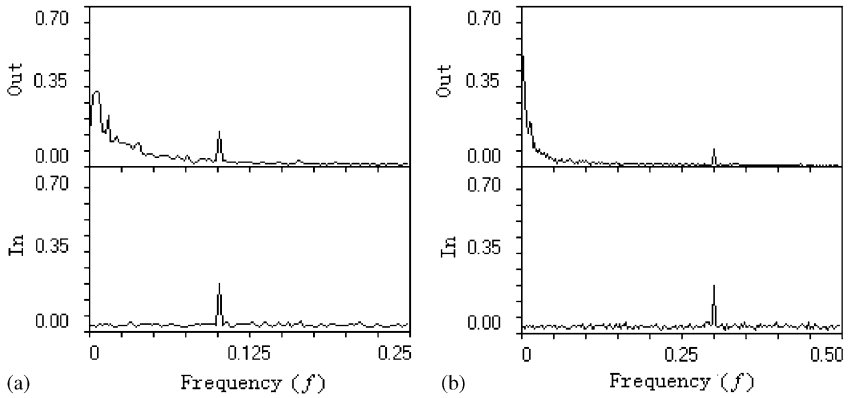

Fig. 4. Spectra of input and output of the bistable system of Eq. (3) for different modulation frequencies: (a) $f_0 = 0.1$ and (b) $f_0 = 0.3$. The other parameters are the same values as in Fig. 3.

It should be noted that in Figs. 3(b) and 4, the input spectral amplitude at f_0 always holds constant no matter how small or big the modulation frequency f_0 is. As we know, this is the usual Fourier transformation property. The clear input spectral spike at f_0 is due to the small noise $D = 0.31$. Hereafter, we will not be interested in the small noise SR, instead we will explore the large noise SR. Our goal is to detect a weak periodic signal submerged in strong noise. When the noise is too strong to distinguish the periodic signal in the input spectrum of a bistable system, we will study a new method to extract or find the periodic signal by means of the SR technique. Large noise does not satisfy the requirement of small noise SR. For example, for the parameters in Fig. 3, the numerical calculation of Eq. (3) will overflow when noise level is increased to a certain value $D = 2.39$. Therefore, we will not be able to use SR directly for larger noise intensity. This result illustrates that the SR phenomenon requires a small parameter noise.

For large frequency and large noise, we note from Fig. 1 that, an SR-like spectral spike at modulation frequency f_0 may be observed if the frequency f_0 is decreased. Such an observation provides us with the possibility of continuing to study the SR with large parameters. We propose the RFSR method in the next section to deal with this issue.

3. Re-scaling frequency stochastic resonance (RFSR)

In practical signal processing, the sampled signal parameters such as the frequency and amplitude of a periodic signal and real noise strength usually exceed the limitation of small parameter SR. Practical signal

parameters are called large parameters. Here it should be noted that the weak signal amplitude and the strong noise intensity may be larger or smaller than one. However, they are just called large parameters if the periodic signal cannot be detected from the noise by the traditional methods, such as direct spectral analysis or averaging.

For example, suppose the practical signal from some types of sensors, for instance, vibration accelerometers, is presented as $sn(t) = A_0 \sin(2\pi f_0 t) + \sqrt{2D}\xi(t)$, where $\xi(t)$ is the zero-mean, one-variance, Gaussian white noise. The total length of data $sn(t)$ is 4000 points. In Eq. (3), let $a = b = 1$, $f_0 = 40$ Hz, $D = 9.1$, $A_0 = 0.3$ (A_0 is still smaller than one). Sampling frequency is selected to be $f_s = 2000$ Hz. Then the time step of numerical calculation is $\Delta t = 1/f_s = 0.0005$ s. The input and output spectra of the bistable system in Eq. (3) are computed with 1024 points FFT and averaged ten times. Fig. 5 shows the numerical results. Here the unit of the output spectral height in Fig. 5(b) is converted to decibel for a clearer display.

It is noted that although we use the average method to analyze the two spectra in Fig. 5(b), the spectral spikes at the driving frequency $f_0 = 40$ Hz in both of the spectra cannot be seen. The input spectrum does not show the weak periodic signal embedded in such heavy noise. Similarly, the output spectrum illustrates that by the direct calculation of Eq. (3) model with large parameters, the weak periodic signal cannot be obtained. This is because the large signal parameters do not satisfy the requirement of the small parameter SR.

In order to detect the weak periodic signal from strong noise by Eq. (3) model, from the discussion in Section 2, we note that the parameter of the driving frequency is the key to deal with the large parameter SR. Since the response amplitude of the bistable system in Eq. (3) can be changed by varying the driving frequency (see Fig. 1), i.e., for fixed modulation amplitude and noise intensity, the smaller the driving frequency, the larger the SR response amplitude. Therefore, based on our earlier work [21], a new method of re-scaling frequency stochastic resonance (RFSR) is proposed: first, the large frequency is compressed linearly according to a proper frequency-scale ratio. The ratio can transform the large frequency into a small parameter frequency; second, the response power spectrum of the bistable system in Eq. (3) is analyzed to pick up the SR-like peak at the compressed signal frequency; and finally, the original large frequency is recovered in accordance with the ratio.

Now we recalculate the previous example (Fig. 5) by the RFSR method. We select the frequency-scale ratio $R = 250$. The compressed driving frequency and the compressed sampling frequency are $f_{0c} = f_0/R = 40/250 = 0.16$ Hz and $f_{sc} = f_s/R = 2000/250 = 8$ Hz, respectively. The time step in the numerical scheme becomes $\Delta t = 1/f_{sc} = 0.125$ s. By re-solving Eq. (3), we obtain the RFSR response of the bistable system shown in Fig. 6. Here for clarity, the display length of the time waveform is 800 points. In the spectrum of Fig. 6, a spectral spike at $f_{0c} = 0.16$ Hz can be distinctly observed, which explicitly indicates the presence of the driving frequency component $f_0 = 40$ Hz. Therefore, the method of the large parameter RFSR provides an effective way to detect a weak periodic signal embedded in heavy noise.

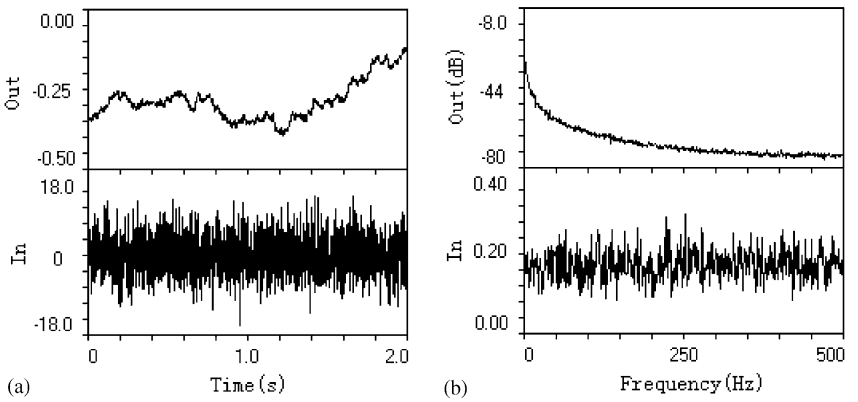

Fig. 5. The input and output of the bistable system in Eq. (3) with large parameters $a = b = 1$, $f_0 = 40$ Hz, $D = 9.1$, $A_0 = 0.3$. (a) Time-domain waveforms. (b) Frequency-domain power spectra.

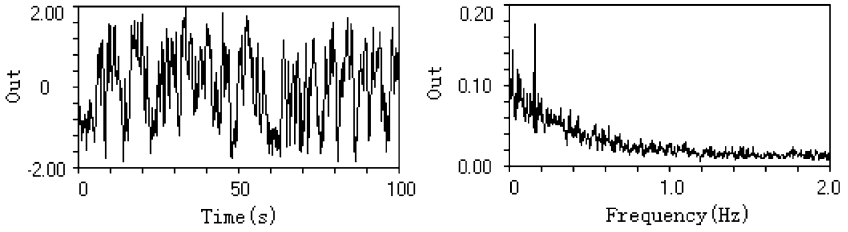

Fig. 6. The output of the bistable system in the model of Eq. (3) with frequency-scale ratio $R = 250$ and time-domain data length 800 points. The other parameters have the same values as in Fig. 5.

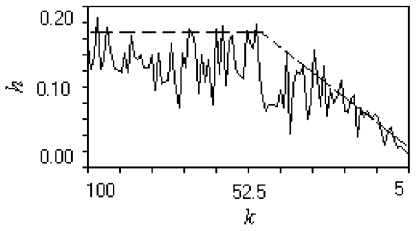

Fig. 7. The signal spectral height h versus k. The other parameters are the same as in Fig. 6.

4. The power spectral behavior of the large parameter RFSR

In practical application, an obvious question is whether the large parameter RFSR can detect distinguishable SR-like spectral peaks at different driving frequencies. From the power spectrum of Fig. 6, we note that the RFSR spectrum has the similar Lorentzian distribution and the noise energy is mainly restricted at the low frequency region where the signal spectral spike is resonated to pop out. This RFSR spectral behavior is consistent with the SR spectral behavior described in Section 2.3. We conclude that the amplitude of the RFSR spectral peak at the driving frequency may decrease with the increase of driving frequency. The question is, how can we quantitatively determine the low frequency region of the large parameter RFSR in which a distinguishable SR-like spectral spike can be detected?

To determine the low frequency region, we take the large parameters of Fig. 6 to study Eq. (3) for a different frequency f_0. Here for convenience, let driving frequency $f_0 = f_s/k$ (or $f_{0c} = f_{sc}/k$). The ratio of the sampling frequency to the signal frequency k ranges from 100 to 5 (i.e., f_0 changes from 20 to 400 Hz for fixed f_s) with an incremental step $\Delta k = -1$. The numerical results for the height h of the RFSR spectral spike at f_0 versus k are shown in Fig. 7.

We see that there exists a critical value around $k = 50$ beyond which the value h keeps relatively large, but below which the value h decreases dramatically. This is basically consistent with the noise energy distribution shown in Fig. 2. The range of $k \geqslant 50$ ($f_0 \leqslant 40$ Hz) corresponds to the low frequency region where an SR-like peak can be easily excited by enough noise, and the range of $k < 50$ ($f_0 > 40$ Hz) overlaps with the higher frequency region where small noise energy can hardly stimulate an SR-like spike. Although there are also several larger peaks in the higher frequency region, $k = 30$ ($f_0 = 66.7$ Hz or $f_{0c} = 0.267$ Hz) for instance (see Fig. 8), these peaks are easily interfered by noise and then may not be identified conveniently.

Therefore, for the maximal detection of SR-like spectral peaks, the low frequency region of the large parameter RFSR should be determined at $k \geqslant 50$. In Fig. 6, the RFSR low frequency region is $f_0 \leqslant 40$ Hz.

It is also noted from Fig. 7 that the curve of h versus frequency f_0 or k has large fluctuations for $k \geqslant 50$. This means that in the RFSR spectrum, some SR-like spectral peaks are distinguishable and some may not. According to the literature [22,23], this actually reflects the selectivity of noise—it is a kind of multi-SR phenomenon. In other words, different noise levels can selectively enhance the signal amplitude at a different signal frequency. This result answers the question at the beginning of this section. That is, the large parameter RFSR can detect distinguishable SR-like spectral peaks at some different driving frequencies.

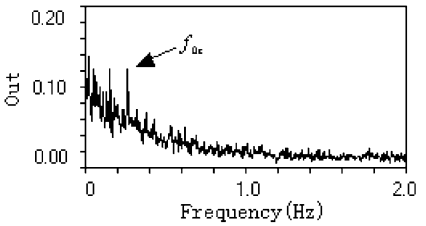

Fig. 8. The output spectrum of Eq. (3) with $k = 30$ or $f_0 = 66.7$ Hz ($f_{0c} = 0.267$ Hz). The other parameters are the same as in Fig. 6.

Table 1
The relationship between D and its minimal $f_{sc\,\min}$

D	$f_{sc\,\min}$	D	$f_{sc\,\min}$
32.0	12.0	6.4	7.0
24.7	11.0	4.0	6.0
18.5	10.0	2.3	5.0
13.5	9.0	1.2	4.0
9.5	8.0	0.5	3.0

The other parameters are the same as in Fig. 6 ($D_{\max} = 32.0$).

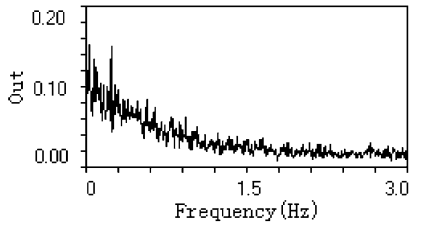

Fig. 9. The output spectrum of Eq. (3) with $D_{\max} = 32.0$ and $f_{sc\,\min} = 12$. The other parameters are the same as in Fig. 6.

The other important spectral behavior of the large parameter RFSR is that the compressed sampling frequency $f_{sc} = f_s/R$ depends on noise intensity D. It is found that each value of noise D has its own minimal compressed sampling frequency $f_{sc\,\min}$. The reason for the existence of $f_{sc\,\min}$ is that the numerical simulation may overflow if $f_{sc} < f_{sc\,\min}$. In general, the RFSR effect with $f_{sc\,\min}$ is better than that with $f_{sc} > f_{sc\,\min}$. However, to obtain a prominent maximal SR-like spectral peak at $f_{0c} = f_{sc\,\min}/k$, there must exist maximal noise intensity $D_{\max}$. When $D > D_{\max}$, for the corresponding $f_{sc\,\min}$, the height of the SR-like spectral spike at f_{0c} is no longer the highest in the whole spectral graph and becomes fuzzy. As an example, Table 1 gives the relationship between D and its corresponding $f_{sc\,\min}$ (reserving one decimal), and Fig. 9 shows the output spectrum of Table 1 at $D_{\max} = 32.0$ and corresponding $f_{sc\,\min} = 12$.

Signal-to-noise (SN) ratio is a useful measure for describing a power spectrum. Similarly, we use the SN ratio to further analyze the RFSR spectral property. According to the literature [24,25], the definition of SN ratio is the ratio of the height of the first harmonic peak in the power spectrum at the signal frequency f_{0c} and the level of the background noise at the same frequency. For the parameters shown in Table 1 and assuming $f_{sc} = f_{sc\,\min}$ for each value of noise D, the variations of the input and output SN ratios of the bistable system in Eq. (3) versus D are shown in Fig. 10. Obviously, the output SN ratio is always larger than the input one. Specifically, when $D \geqslant 3.5$, the values of the input SN ratio begin to be less than 2.1, the minimum of the output SNR. This indicates that with the increase of D, the periodic signal in the input spectrum will be gradually destroyed by the noise and cannot be detected. However, as a result of the RFSR effect, the output SR-like spectral peak keeps its domination to become the maximal distinguishable spectral spike. Therefore,

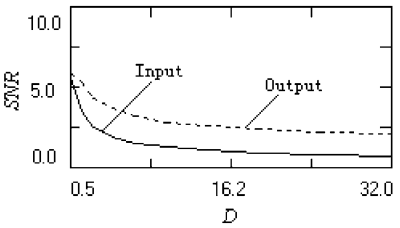

Fig. 10. The input and output SN ratios of the bistable system of Eq. (3) with parameters in Table 1.

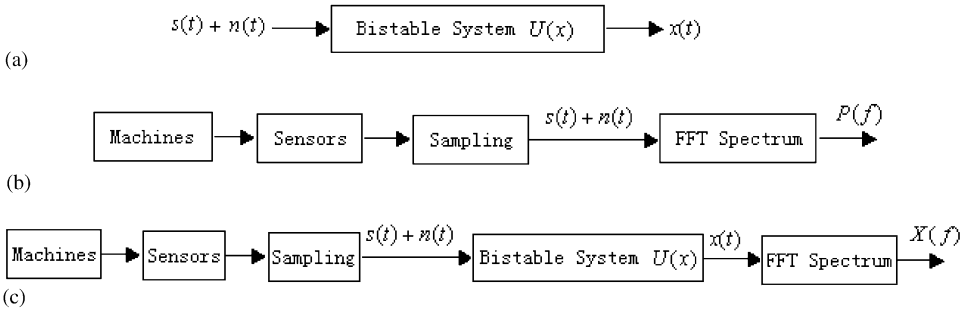

Fig. 11. (a) The model for signal processing based on Eq. (3). (b) The way of conventional fault diagnosis. (c) The combination of Eq. (3) model and the conventional FFT spectrum.

the comparison of input and output SN ratios equally demonstrates the effectiveness of the large parameter RFSR.

5. Discussion of the large parameter RFSR

We know from the above analysis that the one-dimensional dynamic equation (3) is a critical mathematical model to generate the small parameter SR and large parameter RFSR phenomena. Eq. (3) is derived from the motion of a Brownian particle in thermodynamics. It describes the dynamic trajectory $x(t)$ of the particle in a bistable potential function $U(x)$ under the presence of noise $n(t)$ and periodic forcing $s(t) = A_0 \sin(2\pi f_0 t)$. In fact, this model can also be served as a tool of signal processing. It can be understood as the signal processing procedure shown in Fig. 11(a). That is, after the periodic signal $s(t)$ plus noise $n(t)$ passing through the bistable system $U(x)$, the periodic component $s(t)$ can be resonated out at the output $x(t)$ of the bistable system with a proper amount of noise $n(t)$.

In practical application, the recorded data or signal $s(t) + n(t)$ is usually obtained from test and measurement instruments. The recorded data processed by the conventional FFT spectrum analysis is different from the same data processed by the proposed RFSR method. For example, for a mechanical fault diagnosis, a common procedure in the conventional FFT spectrum analysis is plotted in Fig. 11(b). It has been used to monitor and forecast the possible faults of an operating machine. If there exists an early fault in the machine and the measurement noise is so strong that the weak fault signal is submerged in the heavy noise, then the conventional FFT spectrum analysis is hardly to capture the weak fault signal from the spectrum $P(f)$ in Fig. 11(b). Hence, the early fault cannot be found. However, if the large parameter RFSR method is combined with the FFT spectral analysis, the weak fault signal may be extracted from the strong noise. Fig. 11(c) shows such combination. To detect a weak signal embedded in strong noise, according to Fig. 11(c), the RFSR method can be used first to resonate and enlarge the weak signal. Then, the strengthened weak-signal can be detected in the FFT power spectrum $X(f)$.

6. Applications of the large parameter RFSR

In practical engineering measurement and signal processing, to make full use of the RFSR technique to realize the detection of the weak signal, two key parameters, the real sampling frequency f_s and the frequency-scale ratio R, need to be deeply understood. The sampling frequency f_s determines whether the interested signal frequency f_0 is moved into the low-frequency region in which most noise energy concentrates. The ratio R determines whether the large frequency f_0 is scaled into the SR-required small frequency f_{0c}. Only when the detected signal locates in the low frequency region and is driven by small periodic frequency, should a maximal SR-like spectral spike be generated at f_{0c}. Thus, before making data sampling, we should first determine the frequency f_0 of the detected signal. Then, according to Fig. 7, we can decide the practical sampling frequency $f_s \geqslant 50 f_0$. As to the frequency-scale ratio R, since it is not easily determined during the data processing, we directly use the compressed sampling $f_{sc} = f_{sc\,\min}$ rather than the ratio R according to the noise intensity D in Table 1. (Hence, we obtain the ratio $R = f_s/f_{sc}$.) The noise intensity D can be estimated according to the signal correlation. During the calculation of Eq. (3), the f_{sc} obtained through D should be properly adjusted again.

In practical signal processing, the system parameters a and b in Eq. (3) can also improve the RFSR effect. In the previous example, parameters a and b are both equal to one. Thus the height of the potential barrier is constant $\Delta U = a^2/(4b) = 1/4$. If we change system parameters, the height of the potential barrier ΔU will also be changed. By decreasing the height of the potential barrier, the Brownian particle can easily overcome the barrier to form an SR phenomenon. That is, the RFSR effect is improved. Such a case will be illustrated in the following two examples.

6.1. The monitoring and diagnosis of electromotor faults [26]

The first example is the monitoring and diagnosis of the faults of the electromotor in a condensation fan. The fan is monitored and diagnosed periodically with a traditional FFT spectral analysis instrument. Some acceleration sensors used for vibration test are distributed and fixed to the key parts of the equipment. In a routine measurement and analysis, the acceleration power spectrum of the rolling bearing of the fan's electromotor in the vertical vibration direction is shown in Fig. 12(a). The practical sampling frequency is $f_s = 10$ kHz and the recorded data length is 8192 points. The FFT spectrum is calculated with 1024 points and averaged ten times.

In the FFT spectrum, except for some characters of slight scathe of the bearing elements at the frequency 750 Hz and the frequency range from 1300 to 1900 Hz, we cannot see any signs of other faults. When applying the large parameter RFSR technique to this case, we obtain an unexpected RFSR spectrum which is plotted in

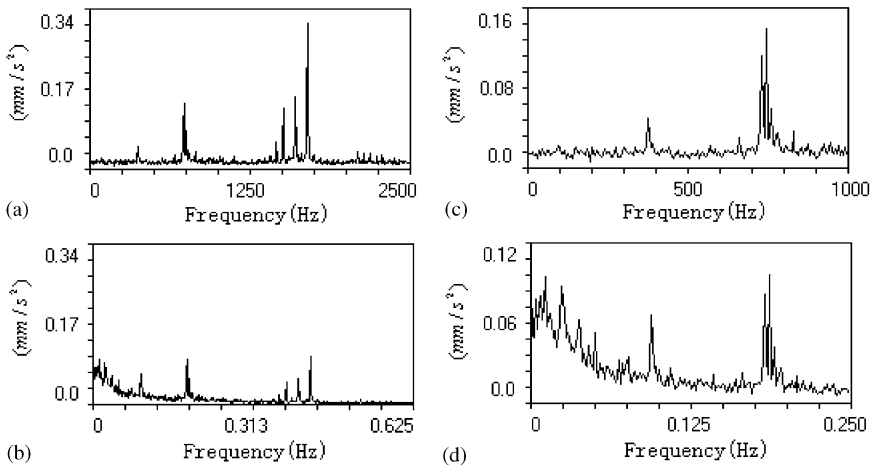

Fig. 12. The rolling bearing acceleration vibration spectrum (a) and its RFSR spectrum (b). For a clear view, (a) and (b) are zoomed in (c) and (d), respectively.

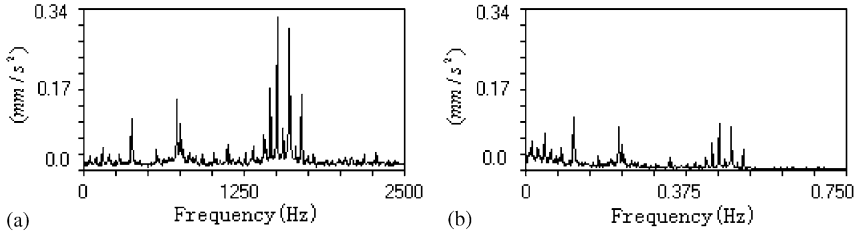

Fig. 13. The rolling bearing acceleration vibration spectrum (a) and its RFSR spectrum (b) obtained after one month.

Fig. 12(b). Some different SR-like spectral peaks regularly emerge at running frequency (i.e., the shaft frequency $f_0 = 50$ Hz) of the rotor and its multiple frequencies (i.e., 100 Hz, 150 Hz, 200 Hz). Here in the calculation of Eq. (3) model, the evaluated noise intensity is $D = 0.227\,\mathrm{mm/s^2}$, the compressed sampling frequency is $f_{sc} = 2.5$ Hz, and the system parameters are $a = 0.4$ and $b = 1$. For a clear display of the low-frequency spectral structure, Figs. 12(a) and (b) are zoomed in Figs. 12(c) and (d), respectively. By the knowledge and experiences of fault diagnosis [27,28], the SR-like spectral spikes at the fundamental frequency and its harmonics may forecast such early mechanical faults in the equipment as rub-impact of the rotor, mechanical looseness, shaft-misalignment, and so on.

To distinguish and confirm what an early fault may exist, the full test of the whole fan was done. The test result exposes that the vibration amplitude of the motor's front-right groundsill is comparatively larger than that of the other parts of the fan, and that the vibration value of the lamina part is very small. Considering the Lorentzian distribution of the spectrum, we think the height difference between the shaft-frequency peak and its harmonic peaks is not large. Thus a primary conclusion is that the possible fault is the mechanical looseness, and that the front-right groundsill of the motor may predicate the looseness position. Since the vibration value is very small, the fan equipment can continue to operate. But it should be closely monitored. Especially, its electromotor should be frequently examined.

One month later, the acceleration vibration power spectrum of the rolling bearing at the same place of the electromotor is demonstrated in Fig. 13(a) again. The practical sampling parameters are the same as stated in Fig. 12. In the vibration spectrum, the spectral peaks at the running frequency and its multiple frequencies appeared. The occurrence of these frequency peaks confirms the existence of the early fault of the mechanical looseness of the fan equipment. These peaks also show the further expansion of the fault after a period of time. The expanded fault is easily obtained by the traditional FFT spectral analysis.

As a comparison, Fig. 13(b) gives the RFSR spectrum corresponding to Fig. 13(a). The relative parameters are $D = 0.418\,\mathrm{mm/s^2}$, $f_{sc} = 3$ Hz, $a = 0.2, b = 1$. Obviously, the spectral peaks at the running frequency and its multiple frequencies in Fig. 13(a) are further amplified by the RFSR. Because the vibration intensity of Fig. 13 is smaller than 1.3 mm/s (by the standard ISO3945) and the vibration amplitude changes little, the mechanical looseness is not so serious and the motor can still continue to work with careful monitoring. In the consequent mid-period examination and maintenance for the condensation fan, the groundsill looseness in the front-right side of the fan's electromotor proves our diagnosis to the fan's fault.

6.2. The vibration analysis of metal cutting process

Another practical instance of applying the large parameter RFSR technique is the vibration signal analysis of the metal cutting process. The experiment is performed at a horizontal numerical control lathe (type: CAK6136P CNC). A piezoelectricity acceleration sensor is fixed at the head of a cutting tool in vertical direction and the signal from the sensor is sampled and recorded in a computer. The sampling frequency is 20.48 kHz and the recorded data is 16384 points. The data length for FFT spectrum calculation is 4096 points and the spectrum is averaged five times. A steel bar, type 45# and diameter ϕ40 mm and hardness HB235, is selected as a test cutting material. The surface of the bar is drilled a blind hole of 6 mm deep and ϕ40 mm in diameter. A piece of column steel, type 40Cr and hardness HB281, is fully inserted into the blind hole. In so doing, the steel-bar becomes an uneven material. Once the cutting tool cuts the hard point of the bar, a

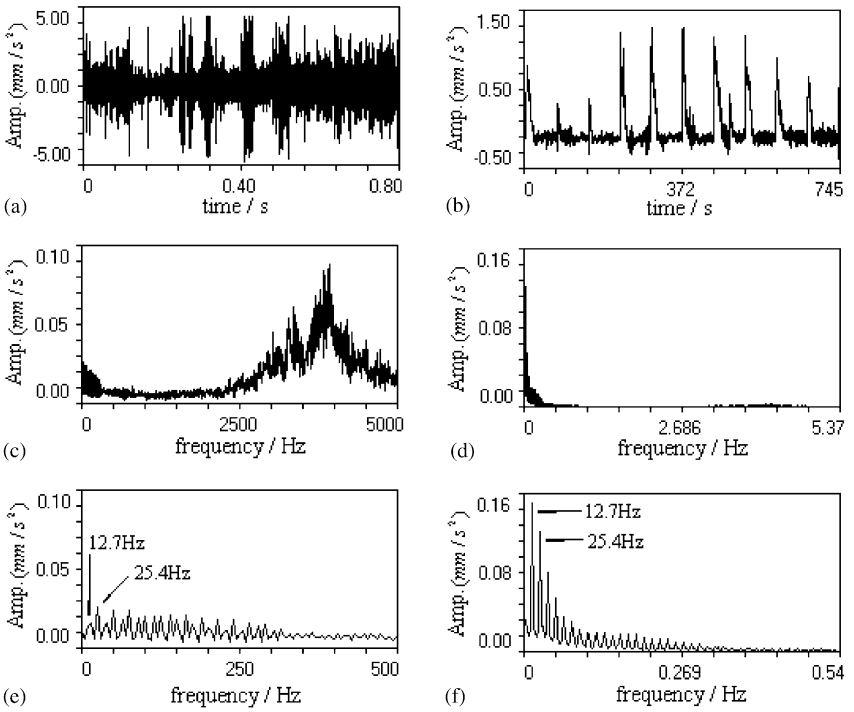

Fig. 14. The time waveforms and the spectra of the cutting vibration. (a) Recorded data waveform. (b) RFSR waveform of the recorded data with $a = 0.1$, $b = 1$ and $f_{sc} = 22$ Hz. (c) Spectrum of the recorded data. (d) Spectrum of the RFSR waveform. (e) and (f) are the low-frequency spectra of (c) and (d), respectively.

periodic pulse vibration will be produced. Obviously, the pulse period or frequency is determined by the rotating speed of the lathe spindle. In the experiment, the real rotating speed of the lathe spindle is 760 rev/min, the feed is 0.1 mm/rev, and the cutting depth is 0.5 mm.

The vibration of the cutting process is depicted in Fig. 14. Figs. 14(a) and (c) show the sampled data waveforms and their frequency spectra, respectively. The time waveform appears in disorder and seems to present a shock in the cutting. The spectrum shows rich vibration property in the low-frequency region and the main mode character of the cutting tool between 3 and 4.5 kHz. Zooming in the low-frequency region (see Fig. 14(e)), we notice that the harmonic frequencies of the fundamental frequency 12.7 Hz extends to more than 300 Hz. The fundamental frequency 12.7 Hz is just the real rotating speed of the lathe spindle 760 rev/min. Fig. 14(e) shows clearly that the cutting process exists periodically with vibration at the period of the rotating speed of the lathe spindle and its harmonics. If the hard point on the surface of the steel-rod is unknown, only by Figs. 14(a), (c) and (e), it is difficult to know what causes the shock waveform in the time domain and harmonic spectrum in the frequency field, and what condition the cutting process may have.

With the large parameter RFSR technique, we obtained the new results shown in Figs. 14(b), (d) and (f). Here the estimated noise intensity is $D = 0.411\,\mathrm{mm/s^2}$, the system parameters are set to $a = 0.1$ and $b = 1$. The compressed sampling frequency is $f_{sc} = 22$ Hz. In Figs. 14(d) and (f), most of the high-frequency mode energy is accumulated in the low-frequency region. This energy accumulation increases drastically the height of the fundamental frequency and its harmonic peaks. The fundamental frequency amplitude becomes the highest spectral spike prior to other harmonic peaks. Meanwhile, in Fig. 14(b), the RFSR time waveform clearly shows the periodic pulses representing the vibration state of the cutting hard point of the steel bar. The width between periodic pulses is just one revolution time span of the lathe spindle $T = 60/760 = 0.079$ s.

7. Conclusions

Conventional SR in signal processing mainly focuses on small parameters, such as rather low frequency and small noise. It has been found that small parameter SR generally does not work well for the case of high-frequency weak signal embedded in strong noise.

In this paper, we first summarize the small parameter SR phenomenon through a simplest bistable system subjected to a weak periodic signal plus small noise. The basic requirement of producing a distinguishable SR spectral spike is that the driving signal frequency should locate at the spectral low-frequency region in which most noise energy concentrates. In order to apply the SR technique to practical large parameter situation, a new approach, the re-scaling frequency stochastic resonance (RFSR) is proposed. The RFSR technique can detect a large-frequency weak signal from heavy noise. Our results show that for the maximal SR-like spectral spike at the driving frequency f_0, the ratio k of the sampling frequency f_s to the driving frequency f_0 should be $k = f_s/f_0 \geqslant 50$. For convenient data processing, the compressed sampling frequency f_{sc} can be determined according to Table 1, and the system parameters a and b can also be adjusted to improve the RFSR effect. The study of the input and output SN ratios of a bistable system demonstrates the effectiveness of the RFSR method, which has been further illustrated by two applications.

Acknowledgments

This research was supported by the Natural Science Foundation of China (No. 50475117) and the Youth Teacher Foundation of Tianjin University (Project No. 5110108).

References

[1] L. Gammaitoni, P. Hänggi, P. Jung, F. Marchesoni, Stochastic resonance, *Reviews of Modern Physics* 70 (1998) 223–287.
[2] A.R. Bulsara, L. Gammaitoni, Turning in to noise, *Physics Today* 49 (1996) 39–45.
[3] X. Godivier, F. Chapeau-Blondeau, Noise-assisted signal transmission in a nonlinear electronic comparator: experiment and theory, *Signal Processing* 56 (1997) 293–303.
[4] S. Zozor, P.O. Amblard, Stochastic resonance in discrete time nonlinear AR(1) models, *IEEE Transactions on Signal Processing* 47 (1999) 108–121.
[5] P. Jung, P. Hanggi, Amplification of small signal via stochastic resonance, *Physical Review A* 44 (1991) 8032–8042.
[6] J.J. Collins, C.C. Chow, T.T. Imhoff, Stochastic resonance without tuning, *Nature* 376 (1995) 236–238.
[7] J.J. Collins, C.C. Chow, T.T. Imhoff, A period stochastic resonance in excitable systems, *Physical Review E* 52 (1995) R3321–R3324.
[8] L. Gammaitoni, Stochastic resonance in multi-threshold systems, *Physics Letters A* 208 (1995) 315–322.
[9] B. McNamara, K. Wiesenfeld, Theory of stochastic resonance, *Physical Review A* 39 (1989) 4854–4869.
[10] M.I. Dykman, R. Mannella, P.V.E. McClintock, N.G. Stocks, Comment on "Stochastic resonance in bistable systems", *Physical Review Letters* 65 (1990) 2606.
[11] G. Hu, H. Haken, C.Z. Ning, A study of stochastic resonance without adiabatic approximation, *Physics Letters A* 172 (1992) 21–28.
[12] L. Gammaitoni, F. Marchesoni, S. Santucci, Stochastic resonance as a *Bona Fide* resonance, *Physical Review Letters* 74 (1995) 1052–1055.
[13] A.L. Pankratov, M. Salerno, Resonant activation in overdamped systems with noise subjected to strong periodic driving, *Physics Letters A* 273 (2000) 162–166.
[14] A.L. Pankratov, Suppression of noise in nonlinear systems subjected to strong periodic driving, *Physical Review E* 65 (2002) 022101_1–022101_3.
[15] R. Li, G. Hu, C.Y. Yang, et al., Stochastic resonance in bistable systems subject to signal and quasimonochromatic noise, *Physical Review E* 51 (1995) 3964–3967.
[16] C. Presilla, F. Marchesoni, L. Gammaitoni, Periodically time-modulated bistable systems: nonstationary statistical properties, *Physical Review A* 40 (1989) 2105–2113.
[17] G. Hu, G. Nicolis, N. Nicolis, Periodically forced Fokker–Planck equation and stochastic resonance, *Physical Review A* 42 (1990) 2030–2041.
[18] L. Gammaitoni, F. Marchesoni, E. Menichella-Saetta, S. Santucci, Stochastic resonance in bistable systems, *Physical Review Letters* 62 (1989) 349–352.
[19] G. Debnath, T. Zhou, F. Moss, Remarks on stochastic resonance, *Physical Review A* 39 (1989) 4323–4326.
[20] T. Zhou, F. Moss, Analog simulations of stochastic resonance, *Physical Review A* 41 (1990) 4255–4264.
[21] Y.G. Leng, T.Y. Wang, Numerical research of twice sampling stochastic resonance for the detection of a weak signal submerged in heavy noise, *Acta Physica Sinica* 52 (2003) 2432–2438.
[22] F. Chapeau-Blondeau, Stochastic resonance at phase noise in signal transmission, *Physical Review E* 61 (2000) 940–943.

[23] J.M.G. Vilar, J.M. Rubi, Stochastic multiresonance, *Physical Review Letters* 78 (1997) 2882–2885.
[24] Z. Gingl, R. Vajtai, L.B. Kiss, Signal-to-noise ratio gain by stochastic resonance in a bistable system, *Chaos, Solitons & Fractals* 11 (2000) 1929–1932.
[25] G.R. Qin, D.C. Gong, G. Hu, X.D. Wen, An analog simulation of stochastic resonance, *Acta Physica Sinica* 41 (1992) 360–369.
[26] Y.G. Leng, T.Y. Wang, R.X. Li, et al., Scale transformation stochastic resonance for the monitoring and diagnosis of electromotor faults, *Proceedings of the Chinese Society of Electrical Engineering* 23 (2003) 111–115.
[27] Y.D. Chen, R. Du, L.S. Qu, Fault features of large rotating machinery and diagnosis using sensor fusion, *Journal of Sound and Vibration* 188 (1995) 227–242.
[28] G.K. Singh, Sa'ad Ahmad Saleh Al Kazzaz, Induction machine drive condition monitoring and diagnostic research—a survey, *Electric Power Systems Research* 64 (2003) 145–158.